Universal quantum computing with correlated spin-charge states

Jordan Kyriakidis
Department of Physics and Atmospheric Science, Dalhousie University, Halifax, Nova Scotia, Canada, B3H 3J5

Guido Burkard
Department of Physics and Astronomy, University of Basel, Klingelbergstrasse 82, CH-4056 Basel, Switzerland

(Dated: February 6, 2008)

We propose a universal quantum computing scheme in which the orthogonal qubit states $|0\rangle$ and $|1\rangle$ are identical in their single-particle spin and charge properties. Each qubit is contained in a single quantum dot and gate operations are induced all-electrically by changes in the confinement potential. Within the computational space, these qubits are robust against environmental influences that couple to the system through single-particle channels. Due to the identical spin and charge properties of the $|0\rangle$, $|1\rangle$ states, the lowest-order relaxation and decoherence rates $1/T_1$ and $1/T_2$, within the Born-Markov approximation, both vanish for a large class of environmental couplings. We give explicit pulse sequences for a universal set of gates (phase, $\pi/8$, Hadamard, CNOT) and discuss state preparation, manipulation, and detection.

PACS numbers: 03.67.Lx, 73.21.La, 85.35.Be

I. INTRODUCTION

Proposals for quantum computing architectures based on semiconductor devices[1,2,3,4,5,6,7] are attractive for their scalability; once the few-qubit problem is solved, massive scalability is not expected to pose insurmountable barriers either in resource requirements or fabrication precision. This is primarily due to the sustained and continued improvements in epitaxy and lithography over the past few decades, and the ability with which new techniques, often developed in industry, are transferred to basic research laboratories. On the other hand, semiconductor environments are hardly systems of pristine quality and isolation, and there are severe trade-offs between long coherence times and short access times.

Pure spin qubits, for example, couple relatively weakly to their environment.[8] Their dipole tails are often negligibly weak and spin exchange effects, while potentially strong, are short range. But precisely because of this weak environmental coupling, spin qubits may be potentially difficult to control and manipulate. For single-particle qubits, local Zeeman tuning is required to rotate bits. The opposite scenario is often true for charge qubits. Here, control may be attained very quickly with metallic gates or optics.[6,7] However relaxation and decoherence times can be very fast, requiring even faster switching times.

This begs the question of whether there exist hybrid qubits which accentuate the positives and mitigate the negatives. We show below that this does indeed seem the case if a single qubit is judiciously defined as a correlated few-body system whose charge and spin degrees of freedom are entangled. These strong correlations should additionally be effective at suppressing relaxation and decoherence through single-particle channels. Indeed our two orthogonal qubit states are identical in their single-particle spin and charge degrees of freedom; differences only show up in their two-body correlation functions.

Sources of decoherence and dissipation can also be broadly classified as spin based or charge based. Both destroy the unitary dynamics of the system either by taking it outside the computational subspace, or by remaining within the computational subspace, but causing either uncontrolled qubit flips, or pure dephasing without dissipation of energy. This will generally occur whenever an environmental influence couples differently to each qubit state. For example, if the two qubit states differ in their spin, then random magnetic fields are an issue. For single-particle qubits, this will always be the case, and likewise for two-particle qubits; it is not possible to define two orthogonal one- or two-particle states with identical spin and charge densities. A three particle system, however, can be constructed in which *both* the charge density and the spin of the two orthogonal $|0\rangle$ and $|1\rangle$ states are identical.

We show that the qubits we define below admit a universal set of one and two-qubit gates, and we give explicit gate pulse sequences which implement this universal set. We also discuss issues of decoherence and relaxation among the qubits and show that, for a broad class of environments, including certain spin dependent ones, relaxation and dephasing are absent ($1/T_1 = 1/T_\varphi = 0$) within the lowest-order Born-Markov approximation. We expect the residual decoherence rate due to higher-order couplings, non-Markovian effects, and other, weakly coupled, environments to be small. We also discuss extensions to the model of system-environment coupling, and comment on issues of state preparation and detection.

In the following section, we describe our model electronic Hamiltonian consisting of two many-body parabolic-elliptic quantum dots, with long-range intradot Coulomb repulsion. In Sec. III we construct our

qubits and demonstrate how correlations produce orthogonal $|0\rangle$ and $|1\rangle$ states with identical spin and single-particle charge densities. Section IV contains explicit implementations—in the form of pulse sequences—for a universal set of quantum logic gates (Hadamard, $\pi/8$, Phase, and CNOT gates). Section V demonstrates that, to lowest order, intra-qubit relaxation and dephasing is absent for all pure spin and pure charge environments which couple to the qubit through single-particle channels. Finally, in Sec. VI, we briefly discuss issues of state preparation and detection.

II. MODEL HAMILTONIAN

We consider two coupled dots with Hamiltonian

$$\hat{H} = \hat{H}_{\rm dot1} + \hat{H}_{\rm dot2} + \hat{H}_{\rm coupl}, \tag{1}$$

where the first two terms denote the individual quantum dots whereas the third denotes interdot coupling. For $\hat{H}_{\rm coupl}$, we shall take a simple coupling Hamiltonian but, within each quantum dot, we shall take full long-range repulsive interactions into account (exactly). We first focus on a single qubit and subsequently discuss two-qubit interactions.

We encode a single qubit in a single elliptically confined[9] two-dimensional lateral quantum dot. We place three interacting electrons in the dot and consider the two-dimensional subspace spanned by the $S = 1/2, S_z = -1/2$ spin sector. Single qubit rotations are created by tuning the eccentricity of the elliptic confinement potential,[10] whereas two-qubit operations, as we show below, are created by controlling the coupling between two adjacent quantum dots.[1,2]

The Hamiltonian of a single dot is given by $\hat{H}_{\rm dot1} = \hat{H}_{\rm 1body} + \hat{H}_{\rm Coul}$, where

$$\hat{H}_{\rm 1body} = \frac{1}{2m}\left(\hat{\boldsymbol{p}} - \frac{e}{c}\hat{\boldsymbol{A}}\right)^2 + \frac{1}{2}m\left(\omega_x^2\hat{x}^2 + \omega_y^2\hat{y}^2\right). \tag{2}$$

We take a magnetic field $\boldsymbol{B} = (0,0,B)$ perpendicular to the plane of the dot. The Hamiltonian (2) can be exactly diagonalized with canonical Bose operators $\hat{a}_1^\dagger$, $\hat{a}_2^\dagger$ and their Hermitian conjugates as[10,11]

$$\hat{H}_{\rm 1body} = \hbar\Omega_+\left(\hat{a}_1^\dagger\hat{a}_1 + \frac{1}{2}\right) + \hbar\Omega_-\left(\hat{a}_2^\dagger\hat{a}_2 + \frac{1}{2}\right), \tag{3}$$

where

$$\Omega_\pm = \frac{1}{2}\sqrt{\omega_0^2 + \omega_c^2 \pm 2\Omega^2}, \qquad \omega_c = \frac{eB}{mc}, \tag{4a}$$

$$\omega_0 = \sqrt{\omega_c^2 + 2\left(\omega_x^2 + \omega_y^2\right)}, \quad \Omega = \left(\omega_-^4 + \omega_c^2\omega_0^2\right)^{1/4}, \tag{4b}$$

$$\omega_- = \sqrt{\omega_x^2 - \omega_y^2}. \tag{4c}$$

We build many-body states through antisymmetrized products of single-particle states $|nm\rangle$, where $\hat{a}_1^\dagger\hat{a}_1|nm\rangle = n|nm\rangle$ and $\hat{a}_2^\dagger\hat{a}_2|nm\rangle = m|nm\rangle$.

The long-range Coulomb interaction $\hat{H}_{\rm Coul}$ can then be written in the usual second-quantized form as

$$\hat{H}_{\rm Coul} = \frac{1}{2}\sum V_{ijkl}c_{i\sigma}^\dagger c_{j\sigma'}^\dagger c_{l\sigma'}c_{k\sigma}, \tag{5}$$

where all indices are summed over. An explicit and exact closed form expression for the matrix element

$$V_{ijkl} = \int d^2q\,\frac{e^2}{2\pi q\varepsilon}(m_in_i, m_jn_j|\mathrm{e}^{i\boldsymbol{q}\cdot(\hat{\boldsymbol{r}}_1-\hat{\boldsymbol{r}}_2)}|m_kn_k, m_ln_l), \tag{6}$$

is derived in Ref. [10].

III. QUBIT CONSTRUCTION

For definiteness, we consider three singly-occupied orbitals $|nm\rangle = |00\rangle,\ |01\rangle,\ |02\rangle$ corresponding to the three lowest-energy orbitals in the lowest Landau level. With this orbital occupation, the $S = 1/2,\ S_z = -1/2$ subspace is two-dimensional and is spanned by our orthogonal qubit states

$$|0\rangle \equiv \frac{1}{\sqrt{6}}\big(2|\downarrow\downarrow\uparrow\rangle - |\downarrow\uparrow\downarrow\rangle - |\uparrow\downarrow\downarrow\rangle\big), \tag{7a}$$

$$|1\rangle \equiv \frac{1}{\sqrt{2}}\big(|\downarrow\uparrow\downarrow\rangle - |\uparrow\downarrow\downarrow\rangle\big). \tag{7b}$$

Each term on the right is a single antisymmetrized state: $|s_0s_1s_2\rangle \equiv c_{00s_0}^\dagger c_{01s_1}^\dagger c_{02s_2}^\dagger|\text{vacuum}\rangle$, where the operator $c_{nms}^\dagger$ creates an electron in state $|nms\rangle$. The spin configurations in Eq. (7) are (up to an overall exchange of spin up and down) those in Ref. [12]; however, the electron states differ in their orbital degrees of freedom. In particular, the states (7) have particles sitting in orthogonal orbitals; this orthogonality is required for the charge densities to be identical during gate operations.

The states in Eq. (7) cannot be written as single Slater determinants in *any* single-particle basis; they are correlated states with entangled spin and charge degrees of freedom. These correlations enable the states to be both orthogonal to each other and yet exhibit identical single particle properties. Both qubit states in (7) have spin $S = 1/2,\ S_z = -1/2$. Furthermore, defining the charge density operator as $\hat{\rho}(\boldsymbol{r}) = \sum_i \delta(\boldsymbol{r} - \hat{\boldsymbol{r}}_i)$, we find $\langle\rho\rangle_{|0\rangle} = \langle\rho\rangle_{|1\rangle} = \sum_i |\psi_{0i}(\boldsymbol{r})|^2$, where $\psi_{nm}(\boldsymbol{r}) \equiv \langle\boldsymbol{r}|nm\rangle$ is a real-space eigenstate of Eq. (2). The density is plotted in Fig. 1 for two different values of $z = \omega_c/\omega_x$.

Physical differences in the qubits arise at the two-body level. For the two-particle density

$$\hat{\rho}_t(\boldsymbol{r}_1, \boldsymbol{r}_2) = \frac{1}{2}\sum_{ij}\delta(\boldsymbol{r}_1 - \hat{\boldsymbol{r}}_i)\delta(\boldsymbol{r}_2 - \hat{\boldsymbol{r}}_j), \tag{8}$$

we find

$$\delta\rho = 2F_{01} - F_{02} - F_{12}, \tag{9}$$

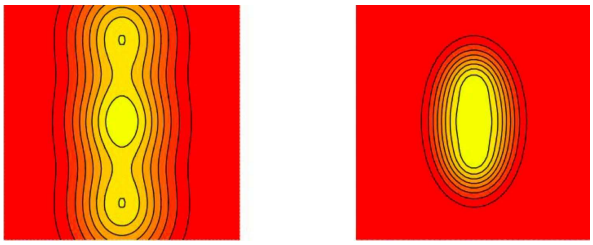

FIG. 1: (Color online) Identical charge density $\langle\rho(\boldsymbol{r})\rangle$ for both qubit states. Both plots have $\omega_y/\omega_x = 1/2$. The left plot is at zero magnetic field whereas the right has $\omega_c/\omega_x = 5$. For $\omega_x = 1$ meV, this corresponds to $B_z \approx 3$ T for GaAs.

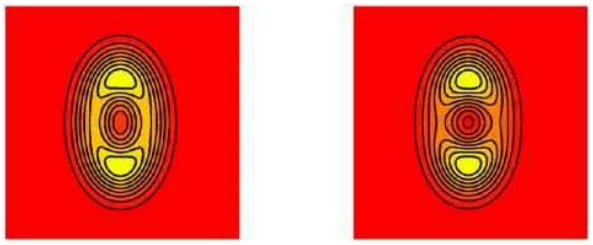

FIG. 2: (Color online) Two-point density $\langle\rho_t(\boldsymbol{r}_1,\boldsymbol{r}_2)\rangle_{|Q\rangle}$ with $\boldsymbol{r}_1 = 0$. The left plot is for $Q = 0$ and the right for $Q = 1$. Both plots have $\omega_y/\omega_x = 1/2$ and $\omega_c/\omega_x = 5$.

where $\delta\rho = \langle\rho_t\rangle_{|1\rangle} - \langle\rho_t\rangle_{|0\rangle}$, and

$$F_{ij} = \mathrm{Re}\left[\psi_i(\boldsymbol{r}_1)\psi_j(\boldsymbol{r}_2)\psi_i^*(\boldsymbol{r}_2)\psi_j^*(\boldsymbol{r}_1)\right]. \qquad (10)$$

The two-point functions are shown in Fig. 2 for $\boldsymbol{r}_1 = 0$.

Because both the single-particle charge and spin properties for both qubit states are identical, intra-qubit decoherence and dissipation should be minimized. We show below that, within the lowest-order Born and Markov approximations, the T_1 and T_2 times are infinite for a very large class of environmental models. Before doing so, however, we first show that a complete universal set of logic gates is achievable in this system.

IV. UNIVERSAL QUANTUM LOGIC GATES

In the space defined by the qubit states in Eq. (7), the electronic Hamiltonian (2) can be written as a pseudospin-1/2 particle in a pseudomagnetic field. In this particular case, we have[10]

$$\hat{H}_{\mathrm{qubit}} = b_x\hat{\sigma}_x + b_z\hat{\sigma}_z + b_0\hat{\sigma}_0, \qquad (11)$$

with $\hat{\sigma}_x$, $\hat{\sigma}_z$ the Pauli spin matrices and $\hat{\sigma}_0$ the identity matrix. The pseudomagnetic field components b_x, b_z, and b_0 are given by

$$b_x = \sqrt{3}\left(V_{0220} - V_{1221}\right)/2, \qquad (12a)$$
$$b_z = -V_{0110} + \left(V_{1221} + V_{0220}\right)/2, \qquad (12b)$$
$$b_0 = V_{0101} + V_{0202} + V_{1212}, \qquad (12c)$$

where V_{ijji} are exchange (and V_{ijij} direct) matrix elements, given in Eq. (6) with $n_i = n_j = 0$, $m_i = i$, and $m_j = j$. Explicit (exact, analytic) expressions of these are given in Refs. [10,13].

The main point with regard to qubit rotations is that the fields in Eq. (12) have a different functional dependence on the dimensionless ratios $r = \omega_y/\omega_x$ and $z = \omega_c/\omega_x$. Thus, adiabatically controlling either $r(t)$ or $z(t)$ can rotate qubits.[14] These ratios may be changed at *fixed* magnetic field (ω_c) by altering the two confinement frequencies ω_x and ω_y independently.

To perform an arbitrary computation, we require a universal set of quantum logic gates which typically consists of both single and double qubit operations. We focus first on the single-qubit portion of this universal set, followed by the two-qubit portion, the CNOT gate.

A. Single Qubit Gates

A universal set[15] of quantum logic gates is given by the CNOT gate, which we discuss below, and the single-qubit Hadamard gate H, $\pi/8$ gate T, and phase gate S. These are each given by

$$H = \frac{1}{\sqrt{2}}\begin{pmatrix}1 & 1\\ 1 & -1\end{pmatrix}, \quad T = \begin{pmatrix}1 & 0\\ 0 & \mathrm{e}^{i\pi/4}\end{pmatrix}, \quad S = \begin{pmatrix}1 & 0\\ 0 & i\end{pmatrix}. \qquad (13)$$

We expect that all SU(2) operations on qubits encoded as in Eq. (7) can be achieved asymptotically since two non-parallel pseudofields are achievable with two different values of r and z.[16]

In order to find explicit time-dependent parameters $r(t)$ and $z(t)$ for which the single-dot time evolution

$$\hat{U} = \widehat{\mathcal{T}}\exp\left(-i\int_0^T \hat{H}_{\mathrm{dot1}}(r(t),z(t))\,dt\right), \qquad (14)$$

equals the desired single-qubit operation, we adapt the minimization method used in Refs. [12,17]. ($\widehat{\mathcal{T}}$ is the time-ordering operator.) The time interval $[0,T]$ is divided into N discrete pieces during which the functions $r(t)$ and $z(t)$ are set constant. We are then left with an optimization problem with $3N$ variables t_i, r_i, and z_i ($i = 1,..,N$) where t_i denotes the length of the ith phase, $\sum_{i=1}^N t_i = T$; the parameters r_i and z_i determine the values of $r(t)$ and $z(t)$ in the ith phase. We numerically minimize the function $f = ||U(\{t_i,r_i,z_i\}) - U_t||^2$ where $U(\{t_i,r_i,z_i\})$ is obtained by exponentiation, Eq. (14), and U_t is the desired target single-qubit operation, Eq. (13).

We have found numerical solutions involving $N = 1$, 3, and 5 steps for the H, T, and S gates respectively. Explicit sequences are shown in Table I,[18] where the time pulse duration is expressed in terms of the dimensionless parameter $\tau = t/t_0$ with $t_0 = (2\pi/\omega_x)[8\pi^2\hbar\omega_x/\mathrm{Ry}]^{1/2}$. Here, $\mathrm{Ry} = m^*e^4/(2\epsilon^2\hbar^2)$ is the effective Rydberg energy, m^* is the effective mass, and ϵ the dielectric constant. For GaAs, Ry $\approx$ 5.93 meV and $t_0 \approx 2.5$ ps for

TABLE I: Pulse sequences for one-bit logic gates. The dimensionless parameters τ, z, and r can be tuned through the time t and any *two* of ω_y, ω_x, and B_z.

Hadamard gate			$\pi/8$ gate			Phase gate		
$2\pi\tau$	z	r	$2\pi\tau$	z	r	$2\pi\tau$	z	r
1.470	0.376	0.158	1.859	4.828	0.022	2.092	0.249	0.121
			3.674	0.102	0.936	1.512	2.803	0.996
			2.443	1.093	0.051	2.123	2.586	0.012
						2.280	0.124	0.916
						1.992	0.224	0.139

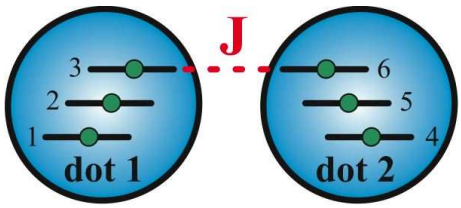

FIG. 3: (Color online) Schematic of our minimal coupling model. As the interdot barrier is lowered, the orbitals highest in energy and with the greatest overlap will be the first to couple.

$\omega_x = 2.5\,\mathrm{meV}$. Note that the sequences shown in Table I are not optimized for experimental efficiency, but merely demonstrate that solutions for a universal set do indeed exist. We have found many more solutions (none shorter) for each of the one-bit gates, including solutions at fixed z.[13]

B. Coupled Dots

To consider two-qubit gates, we now include the interdot coupling term $\hat{H}_{\mathrm{coupl}}$. We consider a minimal model valid in the limit of weak coupling. Of the three orbitals we are considering, the $|nm\rangle = |02\rangle$ orbital is both highest in energy and closest to the edge of the dot. Thus, as the inter-dot barrier is lowered, the respective $|02\rangle$ orbitals in each dot will be the first to couple. This is schematically depicted in Fig. 3. Our minimal model considers the coupling only between these two orbitals. This leads to a Heisenberg form,[1,2]

$$\hat{H}_{\mathrm{coupl}} = J\hat{\boldsymbol{S}}_\ell \cdot \hat{\boldsymbol{S}}_r, \tag{15}$$

where $\hat{\boldsymbol{S}} = \sum_{ss'} c^\dagger_{02s}\boldsymbol{\sigma}_{ss'}c_{02s'}$ is the spin operator of the $|02\rangle$ orbital, and the indices ℓ, r denote the left and right dot respectively.

C. Double Qubit Gate

A two-qubit system is formed from the direct product $|Q\rangle \otimes |Q'\rangle$, of the states in Eq. (7), forming a four-dimensional computational space. The states $|Q\rangle \otimes |Q'\rangle$ are, in fact, $S = 1$, $S_z = -1$ eigenstates. Unfortunately, the spin subspace and the computational subspace are not identical; the six spin (three for each dot) $S = 1$, $S_z = -1$ subspace is nine-dimensional, four of which constitute our $|Q\rangle \otimes |Q'\rangle$ computational space. Thus, our implementation of CNOT, as that in Ref. [12], involves transient excursions outside the computational space; nevertheless, our sequences are designed such that the final gate operation is unitary and returns to the four-dimensional computational space. We require the final state to be such that the CNOT truth table be satisfied, up to single-qubit operations.[19] An explicit implementation is given in Table II. Six parameters are required to describe a pulse: the pulse duration τ, two (r, z) parameters per dot to describe each qubit, and a dimensionless exchange coupling $\mathcal{J} = Jt\hbar/\tau$ describing the coupling. As shown in Table II, a nine step solution is the smallest we have been able to find.[20] (If it were possible to turn off intradot exchange, then a three-pulse CNOT is achievable.[13])

TABLE II: CNOT implementation with an always-on intradot exchange interaction. Subscripts denote individual qubits, $\mathcal{J}$ the interdot exchange, and τ the pulse duration.

$2\pi\tau$	$\mathcal{J}$	z_1	r_1	z_2	r_2
1.227	2.133	0.846	0.630	3.280	0.398
3.821	0.615	1.860	0.067	0.663	0.308
2.766	4.094	0.418	0.767	3.897	0.340
1.167	3.540	0.017	0.298	0.852	0.952
1.591	3.242	1.695	0.370	2.362	0.237
2.148	3.031	2.177	0.559	2.648	0.354
1.560	1.714	3.091	0.077	4.812	0.083
2.255	1.889	1.536	0.222	2.032	0.645
1.981	3.796	21.501	0.453	11.516	0.157

V. DECOHERENCE AND DISSIPATION

Environmental influences can be of two distinct types: Slow variations in the electromagnetic environment merely lead to adiabatic changes in the pseudofield $\mathbf{b}$ and thus to unitary errors that typically average out over the length of a pulse.[14] We look first to fast, non-adiabatic environmental influences that can lead to non-unitary errors—i.e., decoherence—followed by a discussion on adiabatic influences which lead to gate errors.

A. Nonadiabatic Influences

Assuming the environment does not change the number of particles on the dot, and that the bath couples only to single particles in the dot, then a general model

of system-bath coupling is given by

$$\hat{H}_{\rm SB} = \sum \hat{B}^{n'm's'}_{nms}\, c^{\dagger}_{n'm's'} c_{nms}, \qquad (16)$$

where the sum is over all repeated indices. $\hat{B}^{n'm's'}_{nms}$ is a set of arbitrary operators which describe the reservoir and all relevant coupling constants.

At time t, the full state-vector of the system $|\Phi(t)\rangle = \sum_Q |Q\rangle \otimes |\chi_Q(t)\rangle$ ($Q = 0,\ 1$) is a non-separable state, where the states $|\chi_Q(t)\rangle$ are reservoir states including all time-dependent coefficients. Matrix elements of Eq. (16),

$$H^{Q'Q}_{\rm SB} = \sum \langle Q'| c^{\dagger}_{n'm's'} c_{nms} |Q\rangle\, A^{n'm's'}_{nms}(\chi', \chi), \qquad (17)$$

where $A^{n'm's'}_{nms}(\chi', \chi) = \langle \chi' | \hat{B}^{n'm's'}_{nms} | \chi \rangle$ are straightforwardly calculated.[13]

Within the Born-Markov approximation, and using the definitions Eq. (7), the relaxation T_1 and dephasing T_φ times are given by[21,22] ($1/T_2 = 1/(2T_1) + 1/T_\varphi$)

$$\frac{1}{T_1} \sim \left|H^{10}_{\rm SB}\right|^2 = \frac{1}{12}\left|\delta h_0 - \delta h_1\right|^2, \qquad (18a)$$

$$\frac{1}{T_\varphi} \sim \left|H^{00}_{\rm SB} - H^{11}_{\rm SB}\right|^2 = \frac{1}{9}\left|2\delta h_2 - (\delta h_1 + \delta h_0)\right|^2, \qquad (18b)$$

where $\delta h_m = A^{0m\uparrow}_{0m\uparrow} - A^{0m\downarrow}_{0m\downarrow}$. To the extent that the Born-Markov approximation is valid,[23] Eq. (18) states that relaxation and dephasing within the computational space are negligible to leading order for all environmental couplings which are either purely charge or purely spin in character. The former has $\hat{B}^{m'n's'}_{mns} = \delta_{ss'}\hat{B}^{m'n'}_{mn}$ in Eq. (16) and consequently $\delta h_m = 0$, whereas the latter has $\hat{B}^{m'n's'}_{mns} = \delta_{m'm}\delta_{n'n}\hat{B}^{s'}_{s}$ and consequently $\delta h_0 = \delta h_1 = \delta h_2 \neq 0$. For both these cases, dephasing and relaxation vanish within the Born-Markov approximation. (Neither of these is applicable for hyperfine environments which depend on *both* spin and charge.)

B. Adiabatic Influences

Regarding adiabatic (unitary) influences, which do not cause decoherence, these can be minimized by choosing settings for the confinement potential such that $d\boldsymbol{b}/dr$ and $d\boldsymbol{b}/dz$ are small in magnitude. This is the case, for example, for the values $r \approx 0.8$ and $z \to 0$. For these values of the confinement, we find $|d\boldsymbol{b}/dz| \to 0$ and $|d\boldsymbol{b}/dr| \sim e^2/(16\sqrt{2\pi}\lambda)$, where $\lambda^2 = \hbar/(m\omega_x)$. For GaAs material parameters, with $\omega_x = 1$ meV, this gives $|d\boldsymbol{b}/dr| \approx 85\,\mu$eV—at least an order of magnitude smaller than typical pseudofield magnitudes. With these, we can estimate corrections to the adiabatic limit[24] expressed as a leakage time given by $T_{\rm leak} \sim E^4/(\hbar^2 \dot{r}^3 |d\boldsymbol{b}/dr|^2)$, where $E \sim 1$ meV is the excitation energy to states outside the qubit space, and $\dot{r} = dr/dt \sim 10$ GHz is the rate of typical gate operation. For these parameter values, we find $T_{\rm leak} \sim 200\ \mu s$, and a leakage probability of only $P_{\rm leak} \sim 10^{-7}$.

VI. INITIALIZATION AND MEASUREMENT

With regard to state initialization, we note that if the qubit states are the lowest-energy states, then preparation becomes merely a matter of thermalization. In this case, potentials other than elliptic may well prove useful.[9] Ideally, a system where the two qubit states are the two lowest-energy states would be beneficial not only for state preparation, but also for a more general deterrent to dissipation, especially relaxation to states outside the computational basis.

Finally, with regard to measurement, we note that the two states in Eq. (7) are not degenerate. Thus, a destructive measurement is possible by detecting whether a fourth electron resonantly tunnels onto the (three-particle) dot; similarly to the single-shot readout of individual quantum dot spin,[25] the gates may be pulsed such that an additional electron can tunnel onto the dot only if it is in the higher-energy qubit state. In fact, since the tunnel barriers as well as the confinement itself is determined (and controlled) by the applied electrostatic potential, the universal set of gates described above as well as detection may be accomplished using already-existing[8,25] experimental techniques.

Acknowledgments

JK acknowledges support from CFI and NSERC of Canada. GB acknowledges funding from the Swiss SNF and NCCR Nanoscience.

[1] D. Loss and D. P. DiVincenzo, Phys. Rev. A **57**, 120 (1998).
[2] G. Burkard, D. Loss, and D. P. DiVincenzo, Phys. Rev. B **59**, 2070 (1999).
[3] B. E. Kane, Nature **393**, 133 (1998).
[4] F. Troiani, U. Hohenester, and E. Molinari, Phys. Rev. B **62**, R2263 (2000).
[5] E. Biolatti, R. C. Iotti, P. Zanardi, and F. Rossi, Phys. Rev. Lett. **85**, 5647 (2000).
[6] T. Hayashi, T. Fujisawa, H. D. Cheong, Y. H. Jeong, and Y. Hirayama, Phys. Rev. Lett. **91**, 226804 (2003).
[7] X. Li, Y. Wu, D. Steel, D. Gammon, T. H. Stievater, D. S. Katzer, D. Park, C. Piermarocchi, and L. J. Sham, Science **301**, 809 (2003).
[8] J. R. Petta, A. C. Johnson, J. M. Taylor, E. A. Laird, A. Yacoby, M. D. Lukin, C. M. Marcus, M. P. Hanson, and A. C. Gossard, Science **309**, 2180 (2005).
[9] Elliptic confinement is sufficient but not necessary for our

scheme to work. In particular, confinements of less symmetry will certainly also work—purely circular dots will not. The potential essentially should be describable by at least two independent parameters. Elliptic confinement is the simplest such potential.

[10] J. Kyriakidis and S. J. Penney, Phys. Rev. B **71**, 125332 (2005).

[11] A. V. Madhav and T. Chakraborty, Phys. Rev. B **49**, 8163 (1994).

[12] D. P. DiVincenzo, D. Bacon, J. Kempe, G. Burkard, and K. B. Whaley, Nature **408**, 339 (2000).

[13] J. Kyriakidis and G. Burkard, Unpublished (2006).

[14] Changes in the external charge environment are adiabatic if they occur on time scales longer than $\hbar/(e^2/\sqrt{\hbar/m\omega_0})$.

[15] M. A. Nielsen and I. L. Chuang, *Quantum Computation and Quantum Information* (Cambridge University Press, 2000).

[16] D. Stepanenko and N. E. Bonesteel, Phys. Rev. Lett. **93**, 140501 (2004).

[17] G. Burkard, D. Loss, D. P. DiVincenzo, and J. A. Smolin, Phys. Rev. B **60**, 11404 (1999).

[18] Truncating results to (only) three decimal places yields errors in the norm of 0.37%, 1.8%, and 1.4% for the H, T, and S gates respectively.

[19] Y. Makhlin, Quant. Info. Proc. **1**, 243 (2002).

[20] We have found 4 9-step solutions and 25 10-step solutions.

[21] A. Abragam, *The Principles of Nuclear Magnetism* (Oxford University Press, 1961).

[22] A. Khaetskii, D. Loss, and L. Glazman, Phys. Rev. B **67**, 195329 (2003).

[23] D. P. DiVincenzo and D. Loss, Phys. Rev. B **71**, 035318 (2005).

[24] A. Messiah, *Quantum Mechanics* (Dover, 1999).

[25] J. M. Elzerman, R. Hanson, L. H. W. V. Beveren, B. Witkamp, L. M. K. Vandersypen, and L. P. Kouwenhoven, Nature **430**, 431 (2004).